Temperature and concentration dependence of the electrochemical PtHg4 alloy formation for mercury decontamination

Separation and Purification Technology 319 (2023) 124033

Contents lists available at ScienceDirect

Separation and Purification Technology

journal homepage: www.elsevier.com/locate/seppur

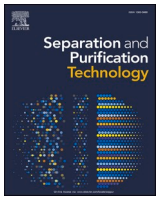

Temperature and concentration dependence of the electrochemical $PtHg_4$ alloy formation for mercury decontamination

Emma Feldt [a], Julia Järlebark [a], Vera Roth [a], Rasmus Svensson [a], Pontus K.G. Gustafsson [a], Nora Molander [a], Cristian Tunsu [b], Björn Wickman [a,*]

[a] Department of Physics, Chemical Physics, Chalmers University of Technology, 41296 Göteborg, Sweden
[b] Department of Chemistry and Chemical Engineering, Nuclear Chemistry and Industrial Materials Recycling, Chalmers University of Technology, 41296 Göteborg, Sweden

ARTICLE INFO

Keywords:
Mercury
Decontamination
Electrochemical alloy
Platinum
$PtHg_4$

ABSTRACT

New and improved methods to remove toxic mercury from contaminated waters and waste streams are highly sought after. Recently, it was shown that electrochemical alloy formation of $PtHg_4$ on a platinum surface with mercury ions from solution can be utilized for decontamination, with several advantages over conventional techniques. Herein, we examine the alloy formation process in more detail by mercury concentration measurements using inductively coupled plasma mass spectrometry in batch measurements as well as electrochemical quartz crystal microbalance analysis both in batch and in flowing water with initial mercury concentrations ranging from 0.25 to 75000 μg L^{-1} Hg^{2+}. Results show that mercury is effectively removed from all solutions and the rate of alloy formation is constant over time, as well as for very thick layers of $PtHg_4$. The apparent activation energy for the electrochemical alloy formation was determined to be 0.29 eV, with a reaction order in mercury ion concentration around 0.8. The obtained results give new insights that are vital in the assessment and further development of electrochemical alloy formation as a method for large scale mercury decontamination.

1. Introduction

Mercury is a toxic heavy metal that poses hazards to all living organisms. [1,2] Mercury and its compounds have been used in many different applications and products, for example: the chlor-alkali process, gold mining, catalysts, dental implants, electrical switches, thermometers and barometers. [3] This has resulted in increased mercury emissions to the environment, especially following the industrial revolution. [4] During the last decades, the use of mercury has largely decreased, but the presence of mercury in the environment and in various industries still remains a large concern in many parts of the world. [5–8].

The high volatility and mobility of mercury is extremely problematic as it causes mercury to continuously cycle in the environment. [9,10] In particular, water bodies have the most significant contribution to the cycling of mercury. As water is vital for living organisms, reducing its contamination with mercury is of critical importance. Mercury is regarded as one of the most toxic threats, which affects the lives of millions of people globally. [7,8] The World Health Organization (WHO) has set a guideline value of mercury for safe drinking water at 6 μg L^{-1} inorganic mercury, [11] and the European Union placed their limit at 1 μg L^{-1}. [12] Decontamination of mercury from wastewaters and natural waters is also an important step in reaching the UN Sustainable Development goals, particularly number 6: Clean water and sanitation.

Various techniques for removal of mercury from water and aqueous streams, e.g. industrial effluents, exist today. [13,14] Notable examples include ion exchange, solvent extraction, coagulation, adsorption and chemical precipitation. [15,16] All of these have specific advantages but also limitations when it comes to efficiency and widespread applicability. Adsorption, e.g. on activated carbon or sulphur based resins such as thiol SAMMs, [17] and sulphide precipitation are simple to use but offer relatively low selectivity for chemically-complex streams that contain multiple heavy metals and are less effective at very low pH; or, in the case of thiol resins, under oxidizing conditions, which oxidize the -SH active sites to disulphide, hindering binding of mercury. Ion

* Corresponding author.
E-mail address: bjorn.wickman@chalmers.se (B. Wickman).

https://doi.org/10.1016/j.seppur.2023.124033
Received 8 March 2023; Received in revised form 19 April 2023; Accepted 4 May 2023
Available online 9 May 2023

exchange and solvent extraction offer better selectivity and high removal efficiency but their cost and difficulties in scale-up limit their applicability at large-scale. Treatment of large volumes of solution with a low mercury concentration is one of the big challenges, as well as finding a method which is easy to regenerate, does not generate complicated secondary wastes, and can recover and isolate the mercury fraction in a very small volume for safe disposal or recycling. We recently presented a new technique for mercury decontamination that could possess all these advantages, including no consumption of chemicals, very high selectivity, low energy cost and large removal capacity. This method is based on electrochemical formation of a very stable alloy between mercury ions in solution and a noble metal, such as platinum, on a cathode electrode. [18,19] The alloy formation process has been shown to be unaffected by the pH of the mercury containing solution in the range 0–6.6, and can be carried out in highly acidic conditions, such as concentrated sulfuric acid. [20] It is also unaffected by the presence of cations such as calcium, cadmium, copper, iron, magnesium, manganese, sodium, nickel, lead and zinc, as well as chloride anions. [19] The process is reversible and allows simple regeneration of the electrode and the re-use the platinum. [19] After the electrodes are saturated with mercury, they can be transferred and regenerated by applying a positive potential in a small volume of solution designed for regeneration purposes. When the regeneration solution reaches a high concentration of mercury, known removal methods such as precipitation can be used to recover the mercury with high purity for safe disposal. Although the electrochemical Pt-Hg system has been described in the past, [21–30] our study was the first to report an application of the $PtHg_4$ electrochemical alloy formation for decontamination of aqueous streams and large-scale decontamination of concentrated sulfuric acid. [19,20] It appears as the process can occur in two main steps: the reduction of mercury ions in solution on the surface of the platinum cathode, according to reaction (1), followed by the formation of the thermodynamically favoured phase $PtHg_4$ according to reaction (2). It should be noted that reaction (2) is most likely composed of a series of reactions and intermediates, such as PtHg and $PtHg_2$. [31] XRD analysis of saturated platinum on glass electrode, identical to the one used in this work and in similar solution, showed that $PtHg_4$ was the predominant phase formed with no clear indications of PtHg and $PtHg_2$. If sufficient bulk mercury is present, as well as sufficient reaction time, $PtHg_4$ is more likely to be formed over the other two phases. [32] The overall reaction can be described with reaction (3). [19,21].

$$Hg^{2+} + 2e^- \rightarrow Hg^0 \quad (1)$$

$$Pt + 4Hg \rightarrow PtHg_4 \quad (2)$$

$$Pt + 4Hg + 8e^- \rightarrow PtHg_4 \quad (3)$$

Most studies so far have focused on characterizing the compounds formed at a platinum interface in contact with liquid metallic mercury [21,29,30] or solutions with very high mercury concentrations (mg – g L^{-1} Hg^{2+}). [24,26,32,33] It is thus unclear if the processes taking place at environmentally relevant concentrations, e.g. if around mg L^{-1} $Hg^{2+}$and lower behave the same and/or if there might be other rate determining steps or mechanisms that dominate the system. For example, at high mercury concentrations, reaction (1) will be much faster than reaction (2), leading to the formation of a layer of metallic mercury on the surface. However, below a certain concentration, reaction (2) will be faster than reaction (1) and the formation of metallic mercury at the surface will be very rare. The kinetics of the alloy formation has previously been investigated on platinum in contact with liquid mercury. [21,30] However, the values reported in different publications for the activation energy differ with as much as 50%. Barlow and Planting [30] found the alloy formation rate to be rather constant over time, with an activation energy of 0.35 eV while Lahiri and Gupta [21] measured an activation energy of 0.52 eV. They also suggest that mercury atoms can easily diffuse through the loosely packed $PtHg_4$ structure and that the reaction is an interface-controlled process at the platinum-alloy interface. In another study by Wu et al., the formation and growth of different Pt-Hg compounds following electrodeposition of mercury ions on a Pt(1 1 1) surface was reported. [33] Only crystalline mercury was found on the surface after deposition of less than one monolayer of mercury. For larger amounts of mercury, the ordered alloys $PtHg_2$ and $PtHg_4$ formed through epitaxial growth. However, the kinetics of the reaction has not been studied for mercury ions electrodeposited on platinum films, and no activation energy has been reported for this system. In present work, we perform batch experiments and electrochemical quartz crystal microbalance (EQCM) measurements in aqueous solutions with a large range of mercury concentrations relevant for environmental and industrial decontamination, spanning five orders of magnitude (0.25–75000 μg L^{-1} Hg^{2+}) and temperatures between 20 and 60 °C. We find an apparent reaction order below one with respect to Hg^{2+} concentration, which signals that the reaction mechanism probably proceed via metallic mercury on the surface. Electrochemical quartz crystal microbalance measurements using flow and batch cells reveal a low activation energy of 0.29 eV and show that the alloy formation rate is unaffected by alloy thickness at least up to several hundred nm in constant mercury concentration. This indicates that the rate limiting step of the process is likely to be the reaction between mercury in the alloy and platinum at the alloy – platinum interface. We also present a mechanistic discussion which provides important information to enable practical use of the technique and brings new knowledge on the processes of electrochemical alloy formation between platinum surfaces and mercury ions in solution.

2. Experimental

2.1. Materials and electrode fabrication

The working electrodes (WEs) for use in batch mode measurements were fabricated as presented in a previous study. [19] Briefly, polished fused silica glass (Mark Optics Inc.) with a thickness of 0.5 mm were cut in 15 × 30 mm pieces and cleaned under sonication, first with acetone, then isopropanol, and finally with pure water. The pieces were used as substrates onto which a 3 nm titanium adhesion layer followed by 100 nm of platinum was deposited using physical vapor deposition (Lesker PVD 225 e-beam evaporator, base pressure ~ 10^{-7} mbar). Deposition masks were used to create a pattern of titanium + platinum consisting of a 15 × 15 mm square at the bottom of the glass substrate with a 1 mm connector strip to the top, where the contact was made. The contact was applied using a polymer-covered copper wire attached with copper conductive tape and sealed with hot glue.

The working electrodes for use in EQCM measurements were fabricated on planar AT-cut quartz crystal sensors without front electrode, with a diameter of 14 nm and basic resonant frequency of 4.95 MHz ± 50 kHz (LAB Analytical, Sweden). The sensors were cleaned by mild oxygen plasma treatment (TePla 300PC, 150 W) for 2 min, and 3 nm Ti/ 200 nm Pt was deposited as a front electrode using the Lesker system described above. A deposition mask was used to create a 5 mm diameter titanium + platinum circle in the middle of the sensor and a 1 mm connector strip to the wrap-around electrode on the side of the sensor.

2.2. Chemicals and electrolyte preparation

Batch setup measurements used an electrolyte consisting of adequate amounts of pure water (MilliQ, Millipore, 18.2 MΩ cm^{-1}), high purity nitric acid solution (65%, Suprapur, Merck), and mercury standard solutions (1000 mg L^{-1}, TraceCERT, Merck). The samples collected from the measurements were diluted for inductively coupled plasma mass spectrometry (ICP-MS) analysis (iCAP Q, Thermo-Fisher) with high purity hydrochloric acid (30%, Suprapur, Merck) containing 2 μg L^{-1} indium as internal standard (10 mg L^{-1} In, CRM, CPAchem). For the EQCM measurements the electrolyte consisted of adequate amounts of

pure water, sulfuric acid (96% Suprapur, Merck), and mercury standard solution (1000 mg L^{-1} Hg^{2+}, TraceCERT, Merck).

It is important to highlight that mercury is a highly toxic chemical and particular care must be used when performing experiments with mercury. Personnel handling the chemicals must use protective equipment to avoid exposure and all materials and chemicals containing mercury must be collected and disposed of in a safe way ensuring that mercury is not released to the environment.

2.3. Electrochemical measurements

For batch measurements, both two-electrode and three-electrode setups were used. A platinum wire (Alfa Aesar, 0.5 mm diameter, 99.95%) was used as a counter electrode (CE) in both cases, and for the three-electrode measurements, a Hg/Hg_2SO_4 electrode (B3610+, SI Analytics) was used as reference electrode. To control the potential and record the current, a potentiostat (Reference 600, Gamry) was used. The potential of the working electrode (WE) was set to 0.16 V vs. the reversible hydrogen electrode (RHE) in the three-electrode measurements. For the two-electrode measurements, a cell voltage of 1.81 V between anode and cathode was applied. The chosen cell voltage was determined from measurements with the reference electrode present and a potential of the WE (cathode) of 0.16 V vs. RHE. The two-electrode measurements were carried out in lower mercury concentrations and here the electrolyte was continuously stirred using a glass covered magnetic stir bar. For the three-electrode measurements carried out in higher mercury concentrations the solution was not stirred.

For each batch experiment, 50 ml 1 mol L^{-1} nitric acid with mercury concentrations varying between 0.25 and 75000 μg L^{-1} was used. The electrodes were fixed so that the solution level was just above the 15 × 15 mm platinum area, and below the contact region, to avoid reactions of mercury with the wire, the copper tape, or the hot glue. The solution level was within ± 1 mm of the thin platinum connection strip.

Samples of the electrolyte were collected before, during, and after electrochemical treatment to monitor the changes in mercury concentration in solution. The volume of samples ranged from 0.05 ml to 2 ml, the larger volume being sampled for the experiments with low initial mercury concentrations. The samples consisting of less than 2 ml were immediately diluted with hydrochloric acid for optimal ICP-MS analysis (the most optimal quantification was attained in a hydrochloric acid matrix). This sampling procedure led to different volumes of the solution being removed for different experiments. For most experiments, less than 7% of the initial volume was removed during the experiment, but for the lowest concentration (0.25 μg L^{-1} Hg^{2+}) the volume removed was as large as 32% (see supplementary information for more information about the sampling procedure).

For the EQCM measurements, two different three-electrode setups were used. In both cases a QSense Explorer was used to analyse the resonance frequencies and a Hg/Hg_2SO_4 electrode (B3610+, SI Analytics) was used as a reference electrode. The potentiostat was the same as the one used in batch measurements and the potential of the WE was set to 0.18 V vs. RHE. The first setup was a flow cell setup consisting of a QSense Electrochemistry Module (QEM 401). The counter electrode consisted of a platinum foil mounted in the ceiling of the measurement chamber in the module and the reference electrode was connected to the electrolyte outflow tube from the module. Approximately 100 ml of the solution was made to continuously flow through the electrochemistry module using a peristaltic pump. The measurements were conducted at different temperatures ranging from 20 to 60 °C, controlled by placing the bulk solution bottle in a water bath with controlled temperature (Julabo F12-ED) and setting the electrochemistry EQCM module to the desired temperature.

The second setup consisted of a sensor holder (QSH-dip, Micro-Vacuum) immersed in a thermostated glass vessel containing 50 ml of electrolyte. The counter electrode was a platinum wire (Alfa Aesar, 0.5 mm diameter, 99.95%). The temperature was controlled by connecting the thermostated glass vessel to the water bath.

For each EQCM measurement, 0.5 mol L^{-1} sulfuric acid with mercury concentration between 100 and 10 000 μg L^{-1} Hg^{2+} was used. The choice of sulfuric acid in the EQCM measurements was due to practical reasons as this electrolyte provided better and more stable electrochemical response in the EQCM setup compared to nitric acid. Previous batch experiments have shown identical mercury removal rates in sulfuric and nitric acids. During the electrochemical treatment, the resonance frequency and higher harmonics (3rd to 7th) were continuously measured. The measured frequency shifts are related to the change in mass of the sensor via the Sauerbrey equation [34]:

$$\Delta f = -\frac{2f_0^2 n}{A_s\sqrt{\rho_q \mu_q}}\Delta m \tag{4}$$

where f_0 is the basic resonant frequency of the sensor before a mass change, n is the overtone number, A_s is the active area, and $\mu_q = 2.947 \times 10^{11}$ g cm^{-1} s^{-2} and $\rho_q = 2.648$ g cm^{-3} are the shear modulus and density of quartz, respectively. The QSense Explorer used also has the ability to measure the energy dissipation for every harmonic. The dissipation can give important information about the viscoelastic properties of and the amount of coupled water on the surface. In our measurements we find a very small shift in dissipation between start and end of the measurement, indicating that both the platinum film and the $PtHg_4$ alloy films formed during experiments are rigid and, thus, the Sauerbrey equation should be valid.

3. Results and discussion

3.1. Mercury removal at different starting concentrations

The decrease in mercury concentration in solution during electrochemical alloy formation in a range of initial concentrations, from 0.25 to 1000 μg L^{-1} Hg^{2+} is shown in Fig. 1. As can be seen, the bulk of mercury is effectively removed from solution in all cases. The rate of mercury concentration decrease is higher for lower initial concentrations. This is most likely explained by the fact that at lower starting concentrations, there is a higher Pt:Hg ratio, and a higher platinum surface area to the amount of mercury atoms (the electrode size, platinum thickness, and initial electrolyte volume were kept constant in all

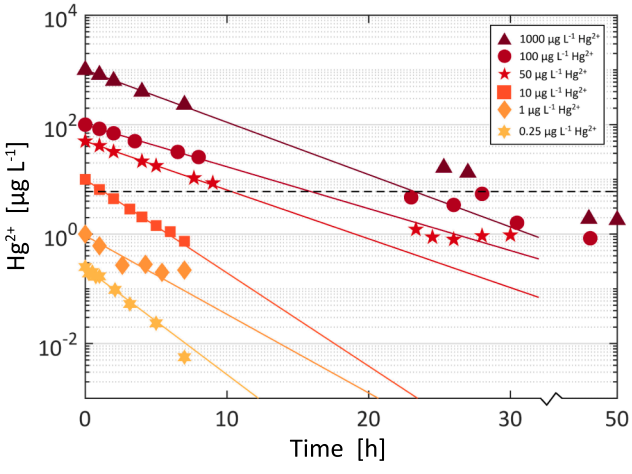

Fig. 1. Mercury concentration in solution versus time of the measurements. The electrolytes for all measurements were 50 ml 1 mol L^{-1} nitric acid solution with initial mercury concentrations 1000–0.25 μg L^{-1} Hg^{2+}. Two-electrode setup, WE: 100 nm platinum film (2.25 cm^2 area), CE: platinum wire. Potential = 0.16 V vs. RHE. The solid lines are exponentially fitted to the experimental data and the black dashed line corresponds to the WHO guideline for safe drinking water, 6 μg L^{-1}.

measurements). At higher concentrations, a full monolayer of alloy is formed relatively fast, whereas at lower concentrations a full monolayer of alloy is never reached. Based on the amount of mercury removed from the experiment with a starting concentration of 1000 μg L^{-1} Hg^{2+}, a full monolayer of $PtHg_4$ is formed within approximately 0.5 h. For the experiments with starting concentrations of 50 μg L^{-1} Hg^{2+} and below, there is less mercury in the solution than would be required to form a full monolayer of $PtHg_4$. Before an alloy monolayer is formed, alloy formation can take place directly at the surface where both platinum and mercury atoms reside after the mercury ions have been reduced (via reaction (1). After a full monolayer of alloy is formed, mercury needs to diffuse through the $PtHg_4$ layer to react with platinum at the platinum – alloy interface. [19] It would not be surprising if these processes occur at slightly different rates.

From the results in Fig. 1 it can also be concluded that all measurements were able, or would be able if they were given more time, to decrease the initial mercury concentration at least two orders of magnitude from the starting concentrations, i.e. removing > 99% of the mercury. For the starting concentrations between 10 and 1000 μg L^{-1} Hg^{2+}, it is interesting to note that the final mercury concentrations are well below the WHO guideline value for safe drinking water (6 μg L^{-1}).

Another central result from Fig. 1 is that electrochemical alloy formation is effective at removing mercury also at the very low starting concentration of 250 ng L^{-1} Hg^{2+}. In this measurement, the mercury concentration decreased to about 6 ng L^{-1} Hg^{2+} in less than 8 h. This is important for practical decontamination and sanitation which often aim at mercury concentrations well below the WHO limit. It should be noted that the thin film working electrodes used here were designed to have high control and to be able to study the electrochemical alloy formation process in detail and not designed for fast mercury uptake. In practice, mercury retrieval will be done using electrodes that allow significantly faster uptake by having a large surface area, e.g., porous electrodes or columns packed with nanoparticles. Copper electrodes, a more abundant and cheaper alternative to platinum, can be used to remove mercury from water, however copper is unstable in oxidizing acids, and without potential control it is also unstable in water. In addition, copper electrodes cannot be electrochemically regenerated and reused. [18] Gold can also be used as an electrode material instead of platinum, as it is well known that gold and mercury form a stable amalgam. However, gold is currently more expensive than platinum and the most stable gold-mercury alloy species is Au_3Hg, which has 12 times less mercury capacity than $PtHg_4$ (per noble metal atom). [35] Less noble metals, such as zinc, aluminium, tin, etc. could potentially also be used, but in practice these metals would likely oxidize and prevent alloy formation and/or be prone to dissolution and degradation. [36,37].

With the current measurement procedures and the detection and quantifications limits of the ICP-MS used, we were not able to conduct experiments with starting concentrations lower than 250 ng L^{-1} Hg^{2+}. However, we expect that the electrochemical alloy formation will remove mercury from solutions also at substantially lower concentrations.

The data presented in Fig. 1 was obtained by performing measurements in a two-electrode configuration. The main reason for this was to keep the system as clean as possible and to avoid potential contamination from or adsorption of mercury in the porous glass frit of the reference electrode. This was found to be extremely important when covering more than four orders of magnitude in concentration and going to sub-μg L^{-1} Hg^{2+} levels. The applied potential between the WE and CE in the two-electrode measurements was established from three-electrode measurements with the WE at 0.16 V vs. RHE. Care was taken to keep a fixed and constant distance between WE and CE in the two-electrode measurement, but it should be mentioned that the actual potential of the WE is less well defined and more difficult to control in a two-electrode setup.

Comparing the rates of mercury removal in the two-electrode measurements presented in Fig. 1 with those obtained in three-electrode configuration (some presented previously19, and more presented in Fig. 2 below), the process is faster in the two-electrode configuration. The reason for this is most likely related to the fact that we chose to use stirring in the two-electrode measurements, which was not the case in the three-electrode measurements. In the concentration range of 50–1000 μg L^{-1} the rate of mercury removal is approximately 3–5 times higher for the two-electrode (with stirring) compared to three-electrode (without stirring) configuration. These results indicate that stirring has a clear effect on the rate of mercury removal from solution, as it increases the transport of mercury ions to the electrode surface. However, very similar results for total amount of mercury removed and dependence on mercury ion concentration at different concentrations were found with and without stirring.

3.2. *Apparent reaction order in Hg^{2+} concentration*

Mercury removal rates in the batch experiments were estimated by calculating the removed mercury from the start of the experiment to the first concentration measurement, usually after 1–2 h, and normalized by the projected area of the electrode. The amount of mercury removed was calculated from the change in concentration, which makes it somewhat uncertain as to which concentration the calculated rate reflects. In the analysis presented below, we have used the initial concentration as a base for the derived rates. We evaluated the strategy to use the average concentration as the base for the derived rates and concluded that the results were not significantly affected. In the EQCM measurements, the rate of mercury uptake is derived directly from the measured frequency shift and as the volume of electrolyte was large compared to the electrode, the mercury concentration was virtually constant during these measurements. The resulting rates from batch experiments with both three- and two-electrode configuration, as well as EQCM measurements are presented in Fig. 2.

From the results in Fig. 2, it is clear that the absolute rate of mercury

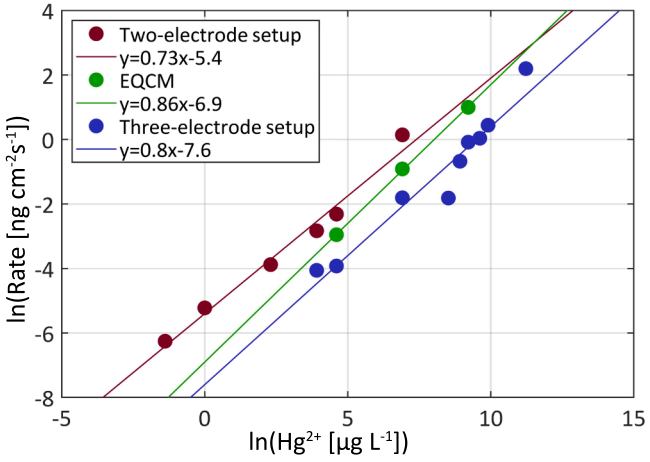

Fig. 2. Natural logarithm of the mercury removal rate versus the natural logarithm of the initial mercury concentrations in the measurements. Red dots: two-electrode batch measurements, blue dots: three-electrode batch measurements, and green dots: EQCM flow cell measurements. For batch measurements, the electrolytes were 50 ml 1 mol L^{-1} nitric acid solution with initial mercury concentrations 1000–0.25 μg L^{-1} Hg^{2+} for the two-electrode measurements and 75,000–50 μg L^{-1} Hg^{2+} for the three-electrode measurements. WE: 100 nm platinum film (2.25 cm^2 area), CE: platinum wire. Reference electrode: Hg/Hg_2SO_4. Potential = 0.16 V vs. RHE. For the EQCM measurements the electrolytes were flowing 0.5 mol L^{-1} sulfuric acid with mercury concentration between 10 000–100 μg L^{-1} Hg^{2+}. WE: Quartz sensor with 200 nm platinum film (0.20 cm^2 area), CE: platinum top wall of the electrochemistry module. Reference electrode: Hg/Hg_2SO_4. Potential = 0.18 V vs. RHE. (For interpretation of the references to colour in this figure legend, the reader is referred to the web version of this article.)

removal is larger for higher initial concentrations, thus, the rate has a clear concentration dependence. To analyse the dependence in more detail, we can first consider the overall reaction (reaction (3). As the surface area of platinum was constant in all measurements of the same type (i.e. batch and EQCM) and the amount of platinum was higher than the amount of mercury removed, we can treat the reaction as being pseudo-first order in platinum and include the platinum concentration in the rate constant. The general rate expression can then be written:

$$r = kC_{Hg^{2+}}^{\alpha} \quad (5)$$

$$\ln r = \ln k + \alpha \ln C_{Hg^{2+}} \quad (6)$$

where r is the rate, k is the rate constant, $C_{Hg^{2+}}$ is the mercury concentration and α is the reaction order in mercury ion concentration. Taking the logarithm of the rate expression makes it possible to determine both the reaction order and the rate constant from a plot of $\ln r$ vs $\ln C_{Hg^{2+}}$, as done in Fig. 2. From analyzing the results in Fig. 2, we determined the apparent reaction order in mercury ion concentration to 0.73, 0.8 and 0.86 for two-electrode, three-electrode and EQCM measurements, respectively. A reaction order below one in Hg^{2+} concentration indicates that the alloy formation is not proceeding directly via Hg^{2+} in solution, as indicated by reaction (3). Instead, it appears likely that the reaction proceeds via formation of metallic mercury on the surface, according to reaction (1), followed by the chemical alloy formation according to reaction (2). If the electroplating of metallic mercury (reaction (1) is faster than the alloy formation (reaction (2), there will be an accumulation of metallic mercury on the surface, which explains the apparent overall reaction order of less than one in Hg^{2+} concentration.

It is interesting to note that despite the fact that the absolute rates differed somewhat between two- and three-electrode setup in the batch experiments, the apparent reaction orders are very similar. It should also be pointed out that the rates presented in Fig. 2 are normalized to projected area. This will not affect the comparison between the batch experiments with two- and three-electrode setup as these were performed with identical electrodes, but for the EQCM measurements a thicker platinum film with a slightly higher roughness was used. The electrochemical surface area (ECSA) of the evaporated platinum films was estimated from hydrogen underpotential deposition (HUPD) by performing cyclic voltammetry in non-mercury, Ar-saturated 0.5 mol L^{-1} H_2SO_4. [38] The roughness factor (i.e. ECSA divided by projected area) was found to be approximately 2.5 for the films used in the batch experiments and approximately 3.3 for the films used in the EQCM experiments.

3.3. Apparent activation energy

Using the EQCM setups, measurements where the temperature was varied between 20 and 60 °C were carried out in order to determine an apparent activation energy of the electrochemical alloy formation. The results are shown in Fig. 3 as an Arrhenius plot with the natural logarithm of the rate of mass increase plotted against the reciprocal of the temperature. Results from both setups are plotted together as they give similar results (see supplementary information for further details). The error bars represent the standard error of the data for each temperature.

From Fig. 3, it is clear that the rate of mercury removal increases with temperature, which also has been observed previously in batch experiments. [19] This is typical for an activated process and as a linear fit follows the data in Fig. 3 rather well, the process can be described by the Arrhenius equation:

$$k = Ae^{\frac{-E_a}{k_B T}} \quad (7)$$

where k is the rate constant, A is a pre-exponential factor , E_a is the activation energy, $k_B = 8.617 \times 10^{-5}$ eV K^{-1} is the Boltzmann constant, and T is the absolute temperature. From Fig. 3, an apparent activation energy for the alloy formation of 0.29 eV and a pre-exponential factor of about 3.0×10^5 ng cm^{-2} s^{-1} are obtained. Previous reports on the solid-state reaction between metallic mercury and platinum have suggested an activation energy of 0.35 [30] and 0.52 [21] eV. Although our value is slightly lower than these, it is quite close to 0.35 eV, which point to that the rate determining step in the solid-state reaction and electrochemical alloy formation from mercury ions could be the same.

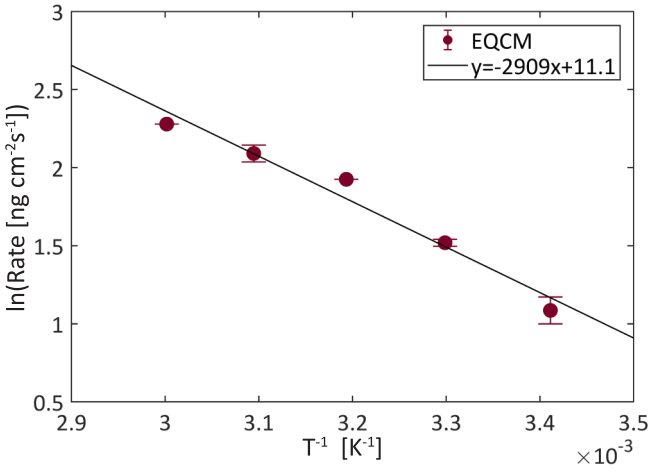

Fig. 3. Arrhenius plot of the data from EQCM measurements at temperatures 20, 30, 40, 50 and 60 °C using both EQCM setups. The electrolytes were 0.5 mol L^{-1} sulfuric acid with mercury concentration 10 mg L^{-1} Hg^{2+}. WE: Quartz sensor with 200 nm platinum film (0.20 cm^2 area). CE: platinum top wall of the electrochemistry module for the flow cell setup and a platinum wire for the dip sensor holder setup. Reference electrode: Hg/Hg_2SO_4. Potential = 0.18 V vs. RHE. The black line is a linear fit to the data.

An activation energy of 0.29 eV is a relatively low value, meaning that the threshold energy needed for the reaction to take place is low. This is important for selective removal of mercury, where the low activation energy means that the process will be favoured instead of other competing reactions. [39].

3.4. Alloy formation in constant Hg^{2+} concentration

Mass change over long time for mercury concentrations of 10 mg L^{-1} Hg^{2+}, 1 mg L^{-1} Hg^{2+} and 100 μg L^{-1} Hg^{2+}, measured with the EQCM flow cell setup, is presented in Fig. 4. The experiments all started with an applied potential of 0.73 V vs. RHE where the $PtHg_4$ alloy formation should not occur. Except for some OH and sub-monolayer platinum oxide formation, no reactions should occur on the electrode and no mass change is expected. As can be seen in Fig. 4, this is also largely reflected in the EQCM data. It can be noted that there is a small background drift in the frequency measurements of roughly 0.1 Hz min^{-1} (corresponding to ~ 0.03 ng cm^{-2} s^{-1}). For the highest concentration in Fig. 4, this drift is negligible, while for the lowest concentration it might constitute up to 60% of the measured signal. At the start of the measurements, the potential of the WE was scanned to 0.18 V vs. RHE where the alloy formation occurs. For all samples, first a small but clear decrease in mass was observed during the scan. The reason for this mass decrease is most likely related to desorption of OH and reduction of platinum oxide. The amount of OH and Pt oxide should be identical on all samples, which is the reason for the relatively large impact from this in Fig. 4C. Short after the potential has reached 0.18 V vs. RHE, a clear mass increase following mercury adsorption and alloy formation is observed. It is interesting to note that during the time at the low potential, the mass increase appears very linear in time, which means that the formation rate of $PtHg_4$ is constant and is not affected by the growing alloy film. This is in good agreement with observations by Barlow and Planting on the metallic mercury – platinum system. [30].

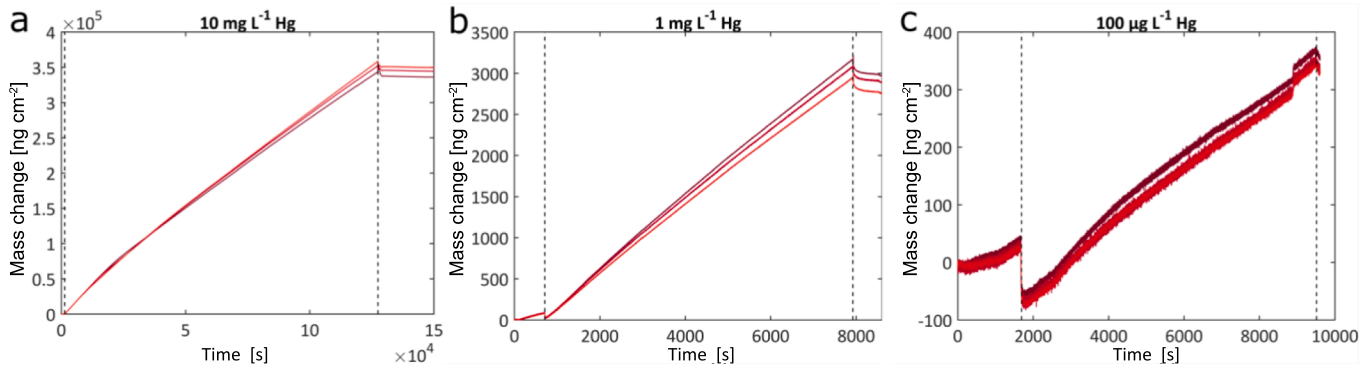

Fig. 4. Calculated mass change from frequency shifts via the Sauerbrey equation. The electrolytes were flowing 0.5 mol L^{-1} sulfuric acid with mercury concentration 10 mg L^{-1} Hg^{2+}, 1 mg L^{-1} Hg^{2+} and 100 µg L^{-1} Hg^{2+}. WE: Quartz sensor with 200 nm platinum film (0.20 cm^2 area). CE: platinum top wall of the electrochemistry module. Reference electrode: Hg/Hg_2SO_4. The dashed lines indicate periods with different potentials applied. Between the dashed lines, 0.18 V vs RHE was applied, and before and after the dashed lines 0.73 V vs. RHE was applied. Harmonics 3, 5 and 7 for the quartz sensor are shown.

To stop the alloy formation in Fig. 4, the potential is scanned back to 0.73 V vs. RHE. As can be seen, this generates a rapid decrease in mass (most pronounced in the low concentration experiment). This is most likely due to a release of metallic mercury attached to the surface of the electrode but not bound in the $PtHg_4$ alloy. A similar effect has been observed before in EQCM for $PtHg_4$ formation. [40] It has been suggested that during the formation of $PtHg_4$, a layer of metallic mercury is formed on the surface, from which mercury atoms can diffuse into the $PtHg_4$ alloy. [22,24,26] By analysing the mass loss at the end of the experiments in Fig. 4, we estimate the mercury layer to be approximately 0.2 nm for the 1 mg L^{-1} Hg^{2+} experiment, which is on the order of one monolayer of mercury. On the 10 mg and 100 µg L^{-1} Hg^{2+} experiments the mercury layer is approximately one order of magnitude higher and lower, respectively. After rapid loss of surface mercury, the mass is constant and, thus, the alloy holding a majority of the absorbed mercury is stable.

Each line in the respective subfigures in Fig. 4 represents the mass calculated from a different harmonic (3, 5, and 7). It can be seen that there is a slight difference in the mass increase for the different harmonics at longer times. This could be due to the different harmonics' radial sensitivity as higher harmonics, are less sensitive to mass changes near the edge of the crystal. [34] Thus, the splitting of the harmonics might be explained by a non-homogeneous alloy formation over the crystal. However, it should be pointed out that the variation between the harmonics as shown in Fig. 4 corresponds to a difference in mass change of less than 5%, indicating a high degree of radial homogeneity of the formed alloy.

3.5. Mechanisms of the electrochemical $PtHg_4$ formation

From the concentration measurements in Fig. 1 and the rate analysis in Fig. 2 it is clear that the reaction rate of the alloy formation is low. Estimating a turnover frequency (TOF) based on the number of mercury atoms removed from solution normalized to the amount of platinum surface atoms gives TOFs of 1.1×10^{-5} and 2.3×10^{-3} at 1 µg L^{-1} Hg^{2+} and 1 mg L^{-1} Hg^{2+}, respectively. These values for TOF are substantially lower than typical values for (electro)catalytic surface reactions. They are however in good agreement with the values presented by Martins et al., where a TOF of around 2×10^{-3} was found for electrochemical reduction in 40 mg L^{-1} Hg on Pt. [32] The low values of the TOF might seem counter intuitive as the applied potential provides a large thermodynamical driving force at the same time as the activation barrier is low. However, it is explained by the very low value of the pre-exponential factor found in the Arrhenius analysis. The reason for the low value of the pre-exponential factor is probably related to the transport of mercury to/in the alloy and/or the reaction mechanism of the alloy formation. There are three steps which can be considered as obvious candidates for rate limiting step, these are illustrated in Fig. 5. The steps are: i) the adsorption and electrochemical reduction of mercury ions on the platinum surface and subsequent insertion into the $PtHg_4$ alloy (Fig. 5a), ii) the diffusion of mercury through the $PtHg_4$ alloy film (Fig. 5b), and iii) the reaction between mercury and platinum at the alloy-platinum interface (Fig. 5c).

We see a clear increase in alloy formation rate when the solution is stirred and, thus, the transport of mercury in solution and the local concentration of Hg^{2+} close to the electrode surface affect the rate. However, it is unlikely that the alloy formation process is limited by the rate of mercury ions reaching the surface as the diffusivity ($D_{Hg^{2+}} = 8.47$ 10^{-10} m^2 s^{-1}) [41] of Hg^{2+} in water is much higher than the reaction rates observed. In addition, the fact that the apparent reaction order in Hg^{2+} is clearly below one indicates that the alloy formation does not proceed directly via Hg^{2+}. Instead, a reaction order below one can be explained by the reduction of Hg^{2+} on the electrode surface being faster than the alloy formation. In this situation, a full or a fraction of a layer of Hg^0 will form on the surface and the alloy formation can proceed. The transport or diffusion of mercury through the alloy appears to be a fast step not limiting the alloy formation under these conditions, as the alloy formation rate in the EQCM measurements revealed a more or less linear mass increase in time, also at a very thick alloy layer (Fig. 4a). Instead, it appears as the rate limiting step is the reaction between mercury and platinum at the alloy-platinum interface. This was also suggested by Lahiri and Gupta[21] to be the rate determining step in the alloy formation of liquid mercury and platinum. Thus, it appears as the reaction mechanism of the electrochemical $PtHg_4$ formation from mercury ions in solution is very similar to the solid-state reaction between liquid mercury and platinum.

4. Conclusions

Measurements of the temperature and concentration dependence in the $PtHg_4$ alloy formation on platinum for mercury decontamination show that the process has an apparent reaction order below one (0.73–0.86) in Hg^{2+} concentration. This is important information for the design of practical decontamination applications to perform well at several or specific mercury concentrations but also for fundamental understanding of the alloy formation process. The fact that the electrochemical alloy formation is effective also from solutions with an initial mercury concentration at least down to 250 ng L^{-1} Hg^{2+} is particularly important for practical applications as it indicates that the process should be able to remove mercury down to extremely low levels. As no indications suggesting a less effective mercury removal were seen at the lowest concentrations of this study, it is likely that the limit for practical mercury removal is on the same order, or potentially even below that of natural waters, which is typically around a few ng L^{-1}.

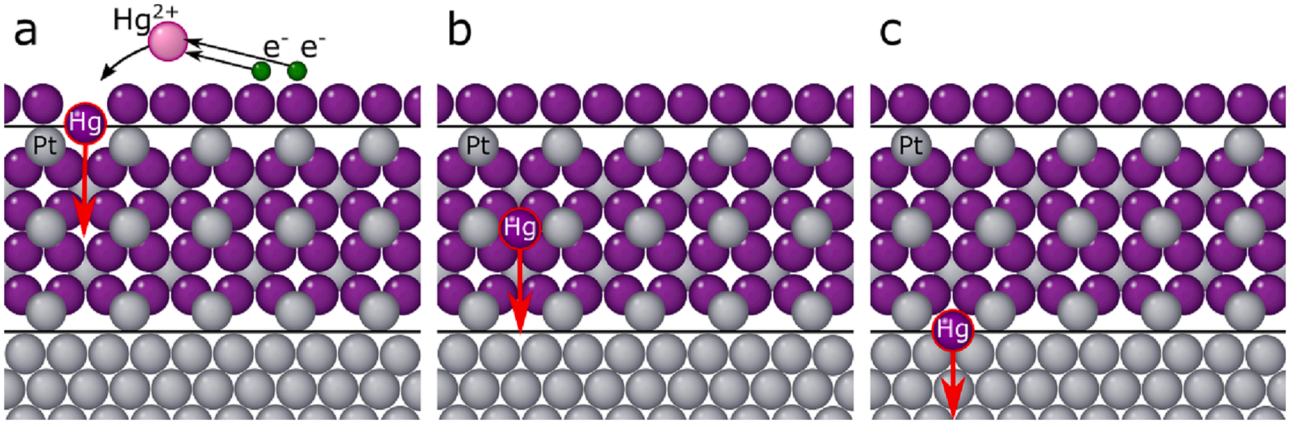

Fig. 5. Illustration of the alloy formation process divided into different stages of the formation. In a), a mercury ion is reduced at the surface and is inserted into the alloy $PtHg_4$ from the surface layer. b) shows how the mercury atom diffuses through the alloy. c) shows the reaction between mercury and platinum at the alloy-platinum interface. Mercury ions (pink), electrons (green), mercury atoms (purple), and platinum atoms (grey). (For interpretation of the references to colour in this figure legend, the reader is referred to the web version of this article.)

This result also agrees well with the finding of a low activation energy of 0.29 eV for the alloy formation process and the high stability of the formed alloy. The activation energy and temperature dependence are central for practical applications, as different types of decontamination, e.g. industrial streams can vary in temperature. Despite the low apparent activation energy, the alloy formation process still has a rather low reaction rate which is explained by the low value of the pre-exponential factor (3.0×10^5 ng cm^{-2} s^{-1}) found in the rate analysis on smooth platinum films. With this information it is possible to design practical electrode systems using high surface or porous electrodes.

Environmental implication

Mercury contamination is a serious problem affecting the environment and threatening the health of humans and animals worldwide. New and improved methods are needed to retrieve mercury from contaminated streams, and to prevent further emissions are needed to mitigate the situation. The mobility and spread of mercury are closely connected to water, which contributes to about 60% to the cycling of mercury in the environment. This study presents fundamental insights to the reaction mechanism, concentration dependance and activation energy of electrochemical alloy formation, a potential future method to decontaminate industrial streams, under relevant conditions.

CRediT authorship contribution statement

Emma Feldt: Investigation, Writing – original draft. **Julia Järlebark:** Investigation, Writing – original draft. **Vera Roth:** Writing – review & editing, Visualization, Data curation. **Rasmus Svensson:** Investigation, Visualization. **Pontus K.G. Gustafsson:** Investigation, Visualization. **Nora Molander:** Investigation. **Cristian Tunsu:** Conceptualization. **Björn Wickman:** Conceptualization, Methodology, Supervision, Funding acquisition, Writing – review & editing.

Declaration of Competing Interest

The authors declare the following financial interests/personal relationships which may be considered as potential competing interests: A patent application (EP 17199244.9) has been filed with C.T. and B.W listed as inventors. Based on the patent, a start-up company (Atium AB) with C.T. and B.W. as minority owners has been formed, with the intention to promote utilization of the results. Proof-of-concept testing has started but no commercial product has yet been released on the market.

Data availability

Data will be made available on request.

Acknowledgements

We acknowledge the Swedish Research Council Formas (project number 2019-01190) for financial support. This work was performed in part at Myfab Chalmers. Rosemary Brown is acknowledged for assisting in the platinum deposition on glass and quartz sensors.

Appendix A. Supplementary data

Supplementary data to this article can be found online at https://doi.org/10.1016/j.seppur.2023.124033.

References

[1] R. Aswathi, K.Y. Sandhya, Ultrasensitive and Selective Electrochemical Sensing of Hg(II) Ions in Normal and Sea Water Using Solvent Exfoliated MoS2: Affinity Matters, J. Mater. Chem. A. Mater 6 (30) (2018) 14602–14613, https://doi.org/10.1039/c8ta00476e.
[2] J.C. Clifton, Mercury Exposure and Public Health. Pediatr. Clin. North Am. 2007, 54 (2), 237-+. Doi: https://doi.org/10.1016/j.pcl.2007.02.005.
[3] T.W. Clarkson, L. Magos, The Toxicology of Mercury and Its Chemical Compounds, Crit. Rev. Toxicol 36 (8) (2006) 609–662, https://doi.org/10.1080/10408440600845619.
[4] B. Bergbäck, U. Lohm, Metals in Society, in: D. Brune, D.V. Chapman, M.D. Gwynne, J.M. Pacyna, (Eds.), The Global Environment: Science, Technology and Management, Wiley-VCH Verlag GmbH, 2008; pp 276-289. Doi: https://doi.org/10.1002/9783527619658.ch16.
[5] A.B. Mukherjee, R. Zevenhoven, J. Brodersen, L.D. Hylander, P. Bhattacharya, Mercury in Waste in the European Union: Sources, Disposal Methods and Risks, Resour. Conserv. Recycl 42 (2) (2004) 155–182, https://doi.org/10.1016/j.resconrec.2004.02.009.
[6] United Nations Environment Programme, Global Mercury Assessment 2013: Sources, Emissions, Geneva, Switzerland, Releases and Environmental Transport; UNEP Chemicals Branch, 2013.
[7] Blacksmith Institute; Green Cross Switzerland, World's. Worst. Pollution. Problems. Report (2010) 2010. http://www.greencross.ch/wp-content/uploads/uploads/media/pollution_report_2010_top_six_wwpp.pdf.
[8] Blacksmith Institute; Green Cross Switzerland, World's. Worst. Pollution. Problems. Report (2016) 2016.
[9] Arctic Monitoring and Assessment Programme. *Arctic Pollution 2011*; Oslo, 2011.
[10] N.E. Selin, Global Biogeochemical Cycling of Mercury: A Review, Annu. Rev. Environ. Resour 34 (2009) 43–63, https://doi.org/10.1146/annurev.environ.051308.084314.
[11] Guidelines for Drinking-Water Quality. 4th Edition, World Health Organization (WHO), Geneva, 2017.
[12] Council Directive 98/83/EC of 3 November 1998 on the Quality of Water Intended for Human Consumption. Official Journal of the European Communities 1998, L 330/32.

[13] D.A. Atwood, M.K. Zaman, Mercury Removal from Water, in: D.A. Atwood (Ed.), Recent Developments in Mercury Science, Springer Berlin Heidelberg: Berlin, Heidelberg, 2006; pp 163-182. Doi: https://doi.org/10.1007/430_013.
[14] A. Sharma, A. Sharma, R.K. Arya, Removal of Mercury(II) from Aqueous Solution: A Review of Recent Work, Sep. Sci. Technol. (Philadelphia) 50 (9) (2015) 1310–1320, https://doi.org/10.1080/01496395.2014.968261.
[15] N. Ariffin, M.M.A. Abdullah, M. R. R. Mohd Arif, Zainol, M.F. Murshed, Z. Hariz, M. A. Faris, R. Bayuaji, Review on Adsorption of Heavy Metal in Wastewater by Using Geopolymer, in: M.A.B. Abdullah, S.Z. AbdRahim, M.E.M. Suandi, M.N.M. Saad, M. F. Ghazali, (Eds.), Engineering Technology International Conference 2016;.; E D P Sciences: Cedex A, 2017; Vol. 97. Doi: https://doi.org/10.1051/matecconf/20179701023.
[16] F.L. Fu, Q. Wang, Removal of heavy metal ions from wastewaters: a review, J. Environ. Manage 92 (3) (2011) 407–418, https://doi.org/10.1016/j.jenvman.2010.11.011.
[17] J. Mattigod, G.E. Fryxell, S. Baskaran, M. Gong, Z. Nie, X. Feng, K.T. Klasson, S. V. ; L. Fabrication and Testing of Engineered Forms of Self-Assembled Monolayers on Mesoporous Silica (SAMMS) Material; USDOE Office of Environmental Restoration and Waste Management, Washington, DC (United States), 1998.
[18] M.K.O. Bengtsson, C. Tunsu, B. Wickman, Decontamination of Mercury-Containing Aqueous Streams by Electrochemical Alloy Formation on Copper, Ind. Eng. Chem. Res 58 (21) (2019) 9166–9172, https://doi.org/10.1021/acs.iecr.9b01513.
[19] C. Tunsu, B. Wickman, Effective Removal of Mercury from Aqueous Streams via Electrochemical Alloy Formation on Platinum, Nat. Commun 9 (2018) 9, https://doi.org/10.1038/s41467-018-07300-z.
[20] V. Roth, J. Järlebark, A. Ahrnens, J. Nyberg, J. Salminen, T. Retegan Vollmer, B. Wickman, Mercury Removal from Concentrated Sulfuric Acid by Electrochemical Alloy Formation on Platinum. *ES&T*, Engineering (2023).
[21] S.K. Lahiri, D. Gupta, A Kinetic Study of Platinum-mercury Contact Reaction, J. Appl. Phys 51 (10) (1980) 5555–5560, https://doi.org/10.1063/1.327440.
[22] M.Z. Hassan, D.F. Untereker, S. Bruckenstein, Ring-Disk Study of Thin Mercury Films on Platinum, J. Electroanal. Chem. Interfacial. Electrochem 42 (2) (1973) 161–181, https://doi.org/10.1016/S0022-0728(73)80390-0.
[23] A.M. Hartley, A.G. Hiebert, J.A. Cox, Preparation and Properties of a Platinum-Based Mercury-Film Electrode, J. Electroanal. Chem. Interfacial. Electrochem 17 (1) (1968) 81–86, https://doi.org/10.1016/S0022-0728(68)80032-4.
[24] F.L. Fertonani, A.V. Benedetti, M. Ionashiro, Contribution to the study of the reaction of mercury with platinum and a platinum-iridium alloy, Thermochim. Acta 265 (1995) 151–161, https://doi.org/10.1016/0040-6031(95)02417-Z.
[25] F.L. Fertonani, A.V. Benedetti, J. Servat, J. Portillo, F. Sanz, Electrodeposited Thin Mercury Films on Pt-Ir Alloy Electrodes, Thin. Solid. Films 349 (1–2) (1999) 147–154, https://doi.org/10.1016/S0040-6090(99)00168-6.
[26] G.R. Souza, I.A. Pastre, A.V. Benedetti, C.A. Ribeiro, F.L. Fertonani, Solid State Reactions in the Platinum-Mercury System, J. Therm. Anal. Calorim 88 (1) (2007) 127, https://doi.org/10.1007/s10973-006-8037-9.
[27] J.R. Turquetti, I.A. Pastre, F.L. Fertonani, Thermal Study of the Solid-State Reactions on Pt-15%Rh/Hg System, Thermochim. Acta 573 (2013) 82–86, https://doi.org/10.1016/j.tca.2013.09.021.
[28] C. Guminski, The Hg-Pt (Mercury-Platinum) System, Bull. Alloy. Phase. Diagrams 11 (1) (1990) 26–32, https://doi.org/10.1007/bf02841581.
[29] G.D. Robbins, C.G. Enke, Investigation of the Compound Formed at a Platinum-Mercury Interface, J. Electroanal. Chem. Interfacial. Electrochem 23 (3) (1969) 343–349, https://doi.org/10.1016/S0022-0728(69)80229-9.
[30] M. Barlow, P.J. Planting, Heterometallic Phenomena in Platinum-Mercury System, Zeitschrift Fur Metallkunde 60 (4) (1969) 292-.
[31] Z. Yoshida, Structure of Mercury Layer Deposited on Platinum and Hydrogen-Evolution Reaction at the Mercury-Coated Platinum-Electrode, Bull. Chem. Soc. Jpn 54 (2) (1981) 556–561, https://doi.org/10.1246/bcsj.54.556.
[32] M.E. Martins, R.C. Salvarezza, A.J. Arvia, The Electrodeposition of Mercury from Aqueous Hg-2(2+) Ion Containing Acid Solutions on Smooth and Columnar-Structured Platinum Electrodes, Electrochim. Acta 43 (5–6) (1998) 549–561, https://doi.org/10.1016/s0013-4686(97)00129-1.
[33] H.L. Wu, S. Yau, M.S. Zei, Crystalline Alloys Produced by Mercury Electrodeposition on Pt(111) Electrode at Room Temperature, Electrochim. Acta 53 (20) (2008) 5961–5967, https://doi.org/10.1016/j.electacta.2008.03.063.
[34] D.A. Buttry, M.D. Ward, Measurement of Interfacial Processes at Electrode Surfaces with the Electrochemical Quartz Crystal Microbalance, Chem. Rev 92 (6) (1992) 1355–1379, https://doi.org/10.1021/cr00014a006.
[35] H. Okamoto, T.B. Massalski, The Au-Hg (Gold-Mercury) System, Bull. Alloy Phase Diagrams 10 (1) (1989) 50–58, https://doi.org/10.1007/BF02882176.
[36] Q. Khan, M.A. Javid, M. Rafique, A. Hussain, K. Nadeem, G. Nabi, K. Mehmood, M. A. -un-Nabi, Synthesis and Mechanical Properties of Dental Amalgam, Mater. Today. Proc 47 (2021) S33–S37, https://doi.org/10.1016/j.matpr.2020.04.672.
[37] U.G. Bengtsson, L.D. Hylander, Increased Mercury Emissions from Modern Dental Amalgams, BioMetals 30 (2) (2017) 277–283, https://doi.org/10.1007/s10534-017-0004-3.
[38] T. Biegler, D.A.J. Rand, R. Woods, Limiting Oxygen Coverage on Platinized Platinum - Relevance to Determination of Real Platinum Area by Hydrogen Adsorption, J. Electroanal. Chem. 29 (2) (1971) 269-, https://doi.org/10.1016/s0022-0728(71)80089-x.
[39] A.L. Petrou, M. Economou-Eliopoulos, The Activation Energy Values Estimated by the Arrhenius Equation as a Controlling Factor of Platinum-Group Mineral Formation, Geochim. Cosmochim. Acta 73 (6) (2009) 1625–1636, https://doi.org/10.1016/j.gca.2008.12.009.
[40] S. Siahrostami, A. Verdaguer-Casadevall, M. Karamad, D. Deiana, P. Malacrida, B. Wickman, M. Escudero-Escribano, E.A. Paoli, R. Frydendal, T.W. Hansen, I. Chorkendorff, I.E.L. Stephens, J. Rossmeisl, Enabling Direct H2O2 Production through Rational Electrocatalyst Design, Nat. Mater 12 (12) (2013) 1137–1143, https://doi.org/10.1038/nmat3795.
[41] D.R. Lide, H.V. Kehiaian, CRC Handbook of Thermophysical and Thermochemical Data, CRC Press, 1994.